Supporting Information

Structural Characterization of Fluoride Species in Shark Teeth

Hsun-Hui Chang,[a] Ming-Jou Chien,[a] Chun-Chieh Kao,[b] Yu-Jo Chao,[a] Pao-Tao Yu,[a] Chun-Yu Chang,[a] Shing-Jong Huang,[c] Yuan-Ling Lee,[b] and Jerry Chun Chung Chan[a]**

[a] Department of Chemistry, National Taiwan University, No. 1, Section 4, Roosevelt Road, Taipei, 10617, Taiwan; [b] Graduate Institute of Clinical Dentistry and School of Dentistry, National Taiwan University and Hospital, No. 1, Chang-Te Street, Taipei, 10048, Taiwan; [c] Instrumentation Center, National Taiwan University, No. 1, Section 4, Roosevelt Road, Taipei, 10617, Taiwan.

Content

1. Experimental Method

Model Compounds. Crystalline samples of HAp (Sigma-Aldrich), CaF_2 (Acros), and KF (Acros) were used as received. The crystalline sample of FAp was prepared as follows. A solution mixture of 0.25 M of EDTA-2Na-Ca (Sigma-Aldrich), 0.15 M of $Na_3PO_4 \cdot 12H_2O$ (Acros), and 0.05 M of NaF (Acros) in DI water was prepared, where the pH was adjusted to 6.0 using HNO_3 and NaOH. The solution mixture was sealed in a Teflon-lined autoclave and aged at 120 ℃ for 24 h. After washing by DI water for three times, the samples were dried at 60 ℃ for 1 day.

Shark Teeth. A head specimen of *Alopias pelagicus* was obtained from a local fish market. There were several series of teeth found on the lower jaw, from which the teeth were removed with surgeon scalpel. No chemical treatment was applied to remove the residual tissues left on the teeth. To prepare teeth samples in powder form, several teeth of similar size and morphology were taken from the outermost series of the anterior region (oA) and were grinded in dry mode (Mixer Mill MM 400, Retsch). The material of grinding tools was zirconium oxide. The oscillation frequency was set to 15 Hz and the grinding time to one minute. The samples were collected by rinsing the grinding tools with DI water under sonication. The sample was subsequently dried by lyophilization. Similarly, other powder samples were prepared from the teeth of the second series (2A), the third series (3A), the fourth series (4A) of the anterior region, and the teeth of the posterior region (P). Note that we did not attempt to separate the dentin and enameloid of our shark teeth samples because of their limited size.

Sample Characterization. Scanning Electron Microscopy (SEM) imaging was carried out on a JEOL-JSM-7600F field emission scanning electron microscope using the backscattering electron mode (BSE). To improve the image resolution, samples

were coated with platinum by Q150R Rotary-Pumped Sputter Coater (Quorum Technologies) under the conditions of low-vacuum (9×10^{-2} mbar) sputter coating at 30 mA. Intact teeth taken from the posterior and anterior regions were embedded in poly(methyl methacrylate) matrix which was prepared by mixing 1.0 g of Tempron (GC) powder and 0.5 mL of liquid. The embedded teeth were then sectioned with PICO 155 Precision Saw (Pace technologies) using diamond wafering blade at a spinning speed of about 600 rpm. X-Ray powder diffraction (XRD) analyses were performed on a PANalytical X'Pert PRO diffractometer using Cu-K_α radiation ($\lambda = 1.5418$ Å), in the 2θ range of 3–60°. FT-IR measurements were conducted on a Nicolet IS5 FT-IR Spectrometer (Thermo Scientific). Raman measurements were performed by InVia Raman microscope (Renishaw) with a Peltier cooled CCD detector. Laser beam for excitation was at the wavelength of 633 nm with maximum laser power of 6.2 mW. The laser beam was directed to the sample through a 20× objective lens to excite the sample and collect signal. The exposure time was set to 10 s throughout the measurements. For the shark teeth sample, the signal enhancement technique of surface-enhanced Raman scattering (SERS) was employed. The ICP-MS measurements were performed on an Agilent 7500ce system. The standard solutions of 1000 mg/L Ca^{2+} and K^+ (Merck) were diluted into ppb levels for the calibration measurements. Selected samples were dissolved in 0.462 mL of 65% HNO_3 and then diluted to a volume of 10 mL with DI water, followed by filtration with 0.22 μm filter.

Solid-state NMR. All ^{19}F direct excitation (Bloch decay) experiments were carried out at the ^{19}F frequency of 600.21 MHz on a Bruker Avance III spectrometer equipped with a commercial 2.5 mm probe. ^{19}F chemical shifts were externally referenced to $CFCl_3$ using CaF_2 powder as the secondary standard (–108.2 ppm). The sample temperature was maintained at 290 K. The ^{19}F direct polarization spectra of teeth samples were

acquired at spinning frequencies from 20 to 30 kHz without proton decoupling. Additional measurements with proton decoupling at 80 kHz gave similar results. The recycle delay was set to 120 s. The ^{19}F spin-lattice relaxation times were determined by the technique of saturation recovery.

$^{19}F\{^{1}H\}$ and $^{31}P\{^{19}F\}$ HETCOR measurements were carried out at ^{1}H, ^{19}F, and ^{31}P frequencies of 600.21, 564.76 and 242.97 MHz, respectively. For the $^{19}F\{^{1}H\}$ HETCOR measurements, the spinning frequency was set to 20 kHz. The CP contact time was 0.5 ms, during which the B_1 field of ^{1}H was linearly ramped from 59 to 66 kHz and that of ^{19}F was empirically optimized. For each t_1 increment, 256 scans were accumulated and a total of 64 increments were acquired at steps of 50 μs. The recycle delay was set to 2 s. For $^{31}P\{^{19}F\}$ HETCOR measurements at 24 kHz, the CP contact time was set to 8 ms, during which the B_1 field of ^{31}P was set to 31 kHz and that of ^{19}F was linearly ramped through the Hartmann-Hahn matching condition. Quadrature detection in the F1 dimension was accomplished by the States-TPPI approach. For each t_1 increment, 128 scans were accumulated and a total of 64 increments were acquired at steps of 20.83 μs. The recycle delay was set to 120 s. ^{31}P and ^{1}H chemical shifts were externally referenced to 85% phosphoric acid and tetramethylsilane (TMS), respectively, using crystalline HAp compound as the secondary standard.

$^{31}P\{^{1}H\}$ HETCOR experiments at the spinning frequency of 20 kHz were carried out at ^{1}H and ^{31}P frequencies of 400.13 and 161.98 MHz, respectively, on a Bruker Avance III spectrometer equipped with a 2.5 mm probe. During the contact time period, the ^{1}H nutation frequency was set to 50 kHz and that of ^{31}P was ramped linearly through the Hartmann-Hahn matching condition. Two-pulse phase-modulation (TPPM)[1] proton decoupling of 75 kHz was applied during the acquisition period. For each t_1 increment, 32 scans were accumulated and a total of 64 increments were acquired at steps of 100 μs.

A series of HETCOR experiments were carried out with contact time varied from 0.3 to 18 ms for the teeth samples.

For the measurements of $^{31}P\{^{19}F\}$ transfer echo double resonance (TEDOR) spectra,[2] the spinning frequency was 24 kHz; the optimized in-phase to anti-phase conversion time one rotor period, and the B_1 fields of all $\pi/2$ pulses 50 kHz. The recycle delay was set to 10 s. The initial ^{19}F polarization was created by direct excitation.

2. Figures

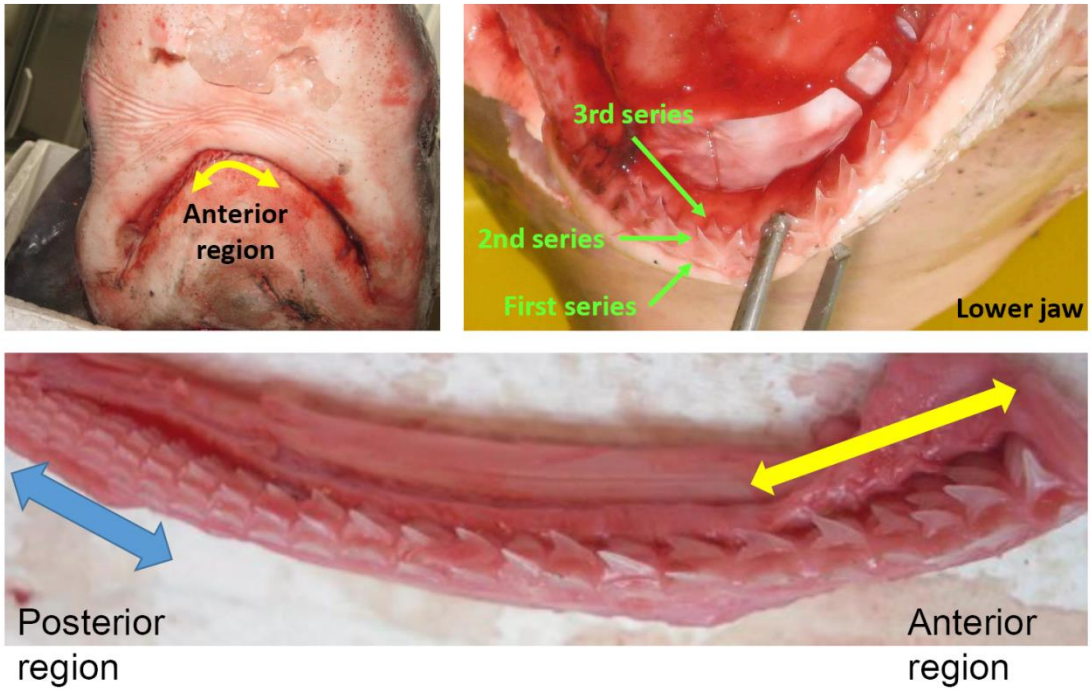

Figure S1. Illustration of the anterior and posterior regions of shark teeth studied in this work. The fourth-series teeth in the anterior region (4A) were backed onto the gum tissues.

(a)

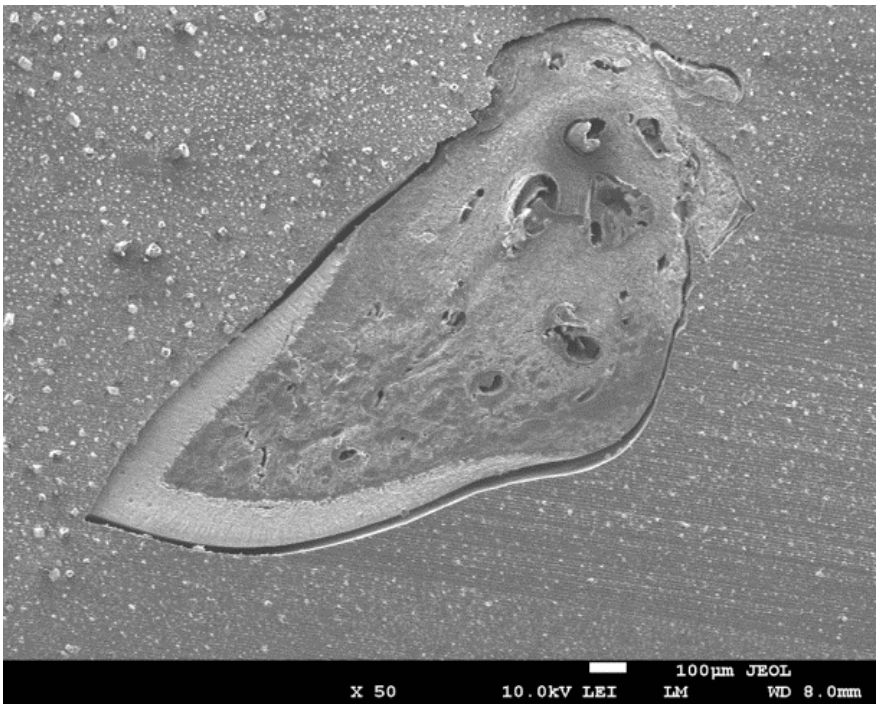

(b)

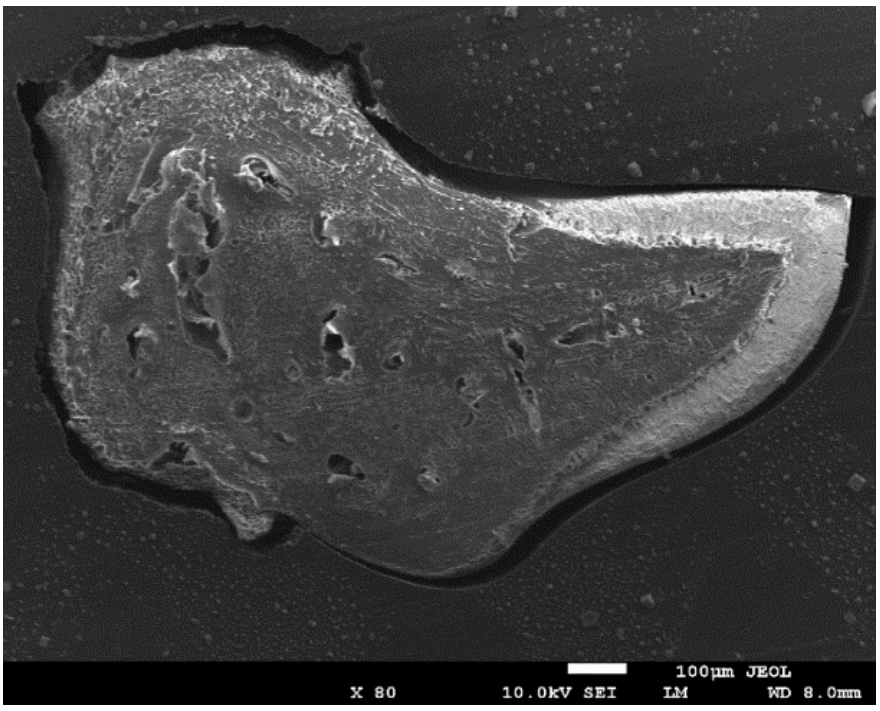

Figure S2. SEM images in backscattering electron mode of (**a**) an outer anterior tooth and (**b**) a posterior tooth.

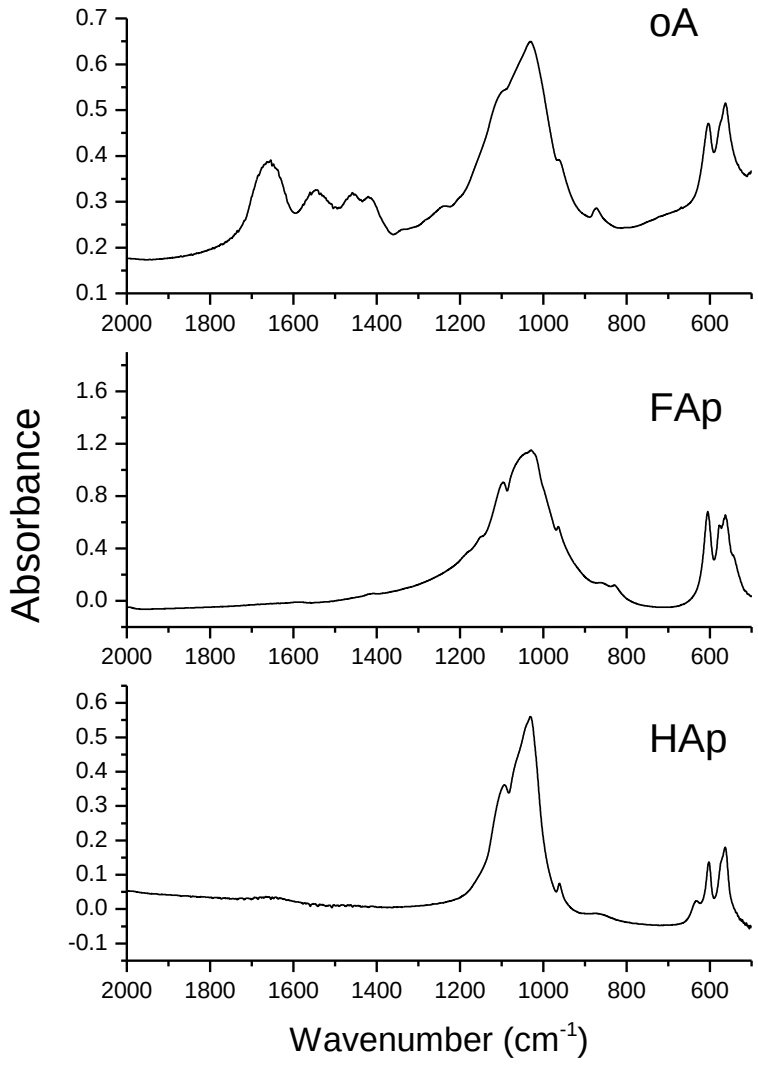

Figure S3. FTIR spectra of the outer anterior (oA) teeth and model compounds. Characteristic absorption peaks of apatite include the O-H bending (632 cm^{-1}), O-P-O bending (563, 605, and 962 cm^{-1}) and the antisymmetric P-O stretching (1030 and 1092 cm^{-1}).[3,4] Three additional peaks observed for shark teeth sample only are 1415 cm^{-1} for ν_3 mode of CO_3^{2-}, 1550 and 1667 cm^{-1} of amide-I absorbance bands.[5] The peak at 1667 cm^{-1} could either be due to the $-COO^-$ vibration[6] or the structural water of ACP.[3]

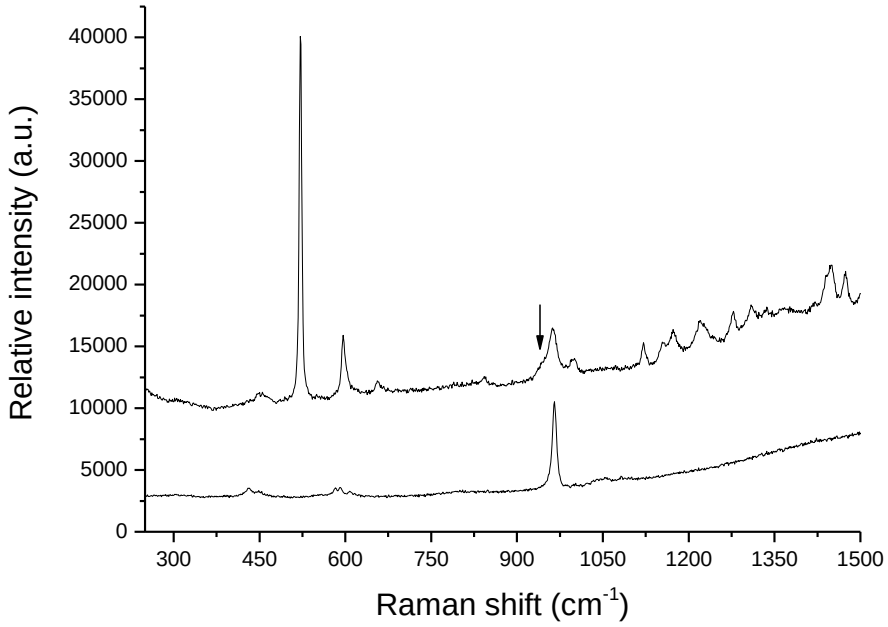

Figure S4. Raman spectra of the oA sample (upper trace) and the HAp sample (lower trace). Typical vibrational modes of apatitic PO_4^{3-} include ν_1 (960 cm^{-1}), ν_2 (430 cm^{-1}), and ν_4 (591 and 655 cm^{-1}).[3,7] For the oA spectrum, the shoulder at around 950 cm^{-1} (indicated by an arrow) was assigned to ACP. For the teeth sample, the absorption at 520 cm^{-1} is the background signal of silver-coated tapered silica nanopillar for surface-enhanced Raman scattering.

(a)

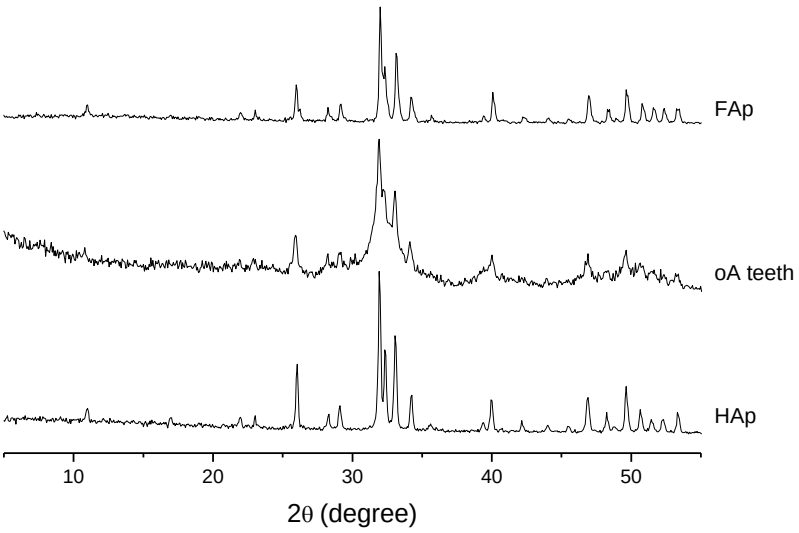

(b)

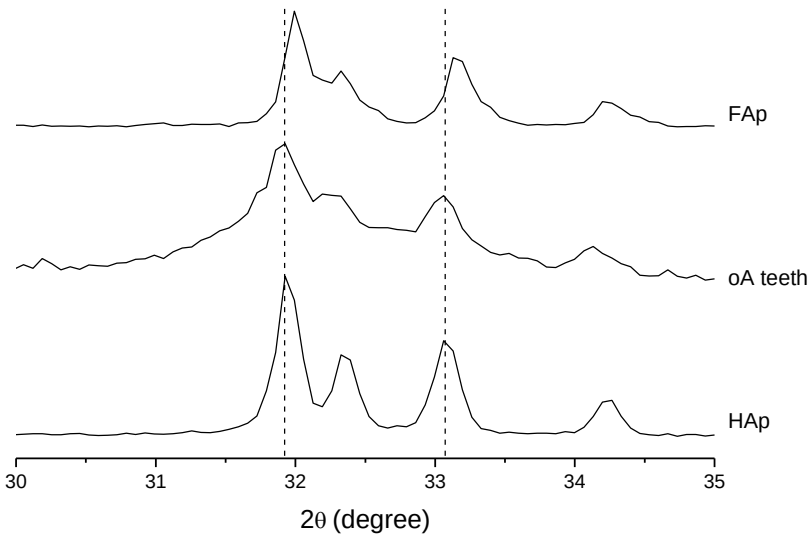

Figure S5. XRD patterns of the outer anterior teeth (oA) sample and the crystalline compounds of FAp and HAp. (**a**) Full pattern. (**b**) Expanded region from 30 to 35 deg.

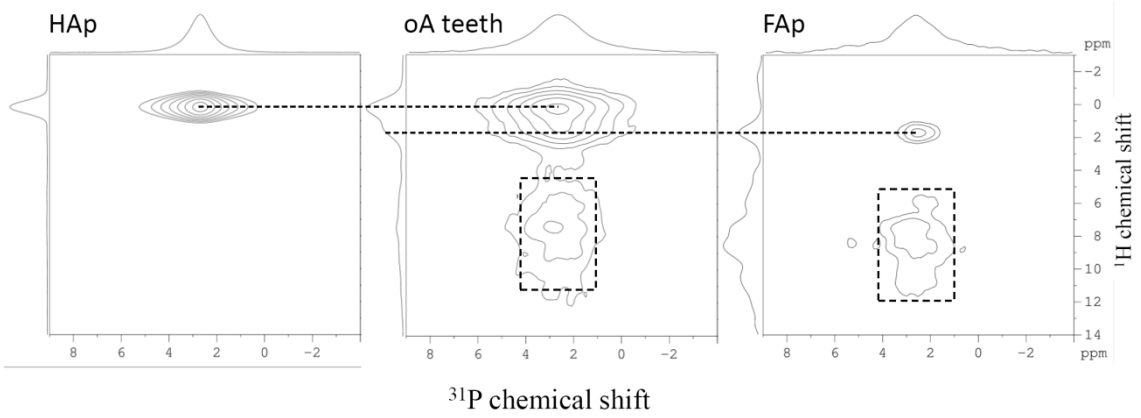

Figure S6. $^{31}P\{^{1}H\}$ HETCOR spectra acquired for the outer anterior shark teeth and the model compounds of HAp and FAp. Although pure FAp will not give any signal in a $^{31}P\{^{1}H\}$ HETCOR spectrum, the correlation peak observed for the FAp sample indicated that some fluoride sites of FAp were replaced by OH groups. In other words, our FAp sample contained minor fraction of hydroxyfluorapatite (HFAp). The observed correlation peak at 2.6 ppm (^{31}P)/1.8 ppm (^{1}H) was assigned to the PO_4^{3-}/OH^- correlation peak of HFAp. Subsequent spectral deconvolution of the ^{19}F MAS spectrum of the model compound FAp reveals that the fraction of HFAp is about 16.8 wt%. The broad peaks enclosed in the dashed rectangles were assigned to ACP. The apatite region of the oA teeth included both the HAp and HFAp signals. The corresponding signal region was defined from −1 to 6 ppm and from 0 to 3 ppm of the ^{31}P and ^{1}H dimensions, respectively.

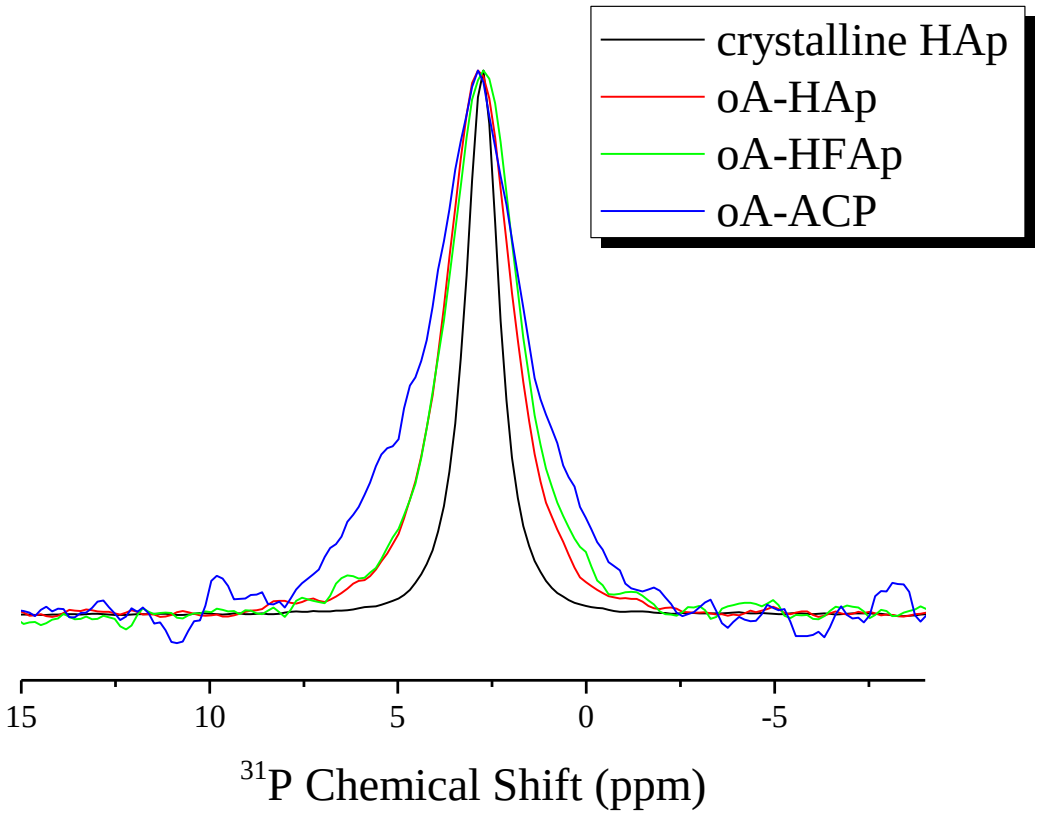

Figure S7. Projections of the $^{31}P\{^{1}H\}$ HETCOR spectrum acquired for the oA and HAp samples (Figure S6). As expected, the line width at half maximum of the ACP component is larger than those of the HAp and HFAp components.

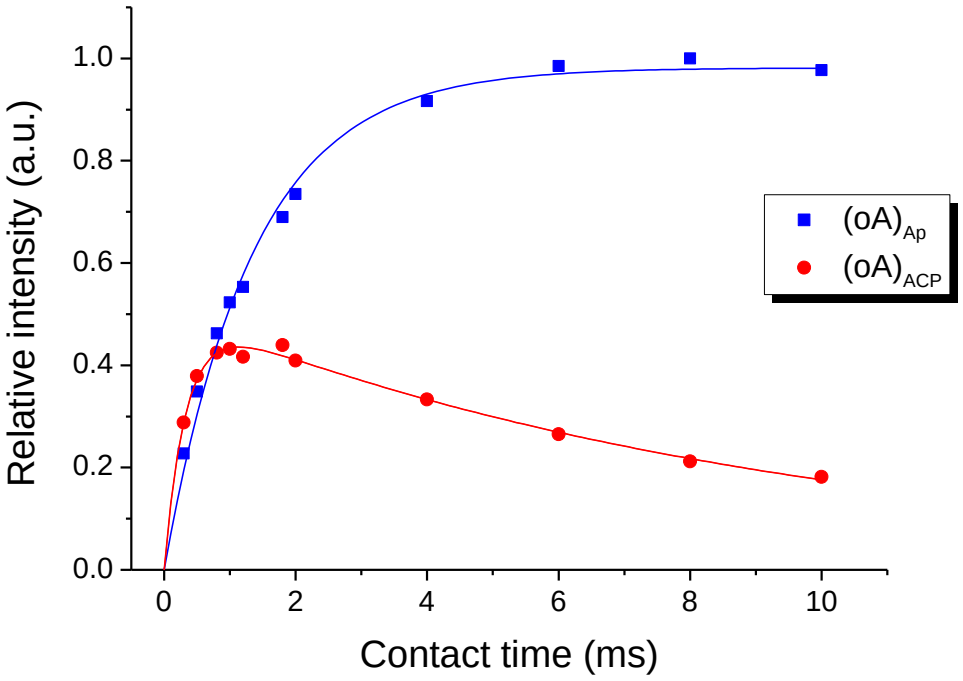

Figure S8. $^{13}C\{^{1}H\}$ variable contact-time CPMAS results obtained for the oA teeth. The red dots represented the signal integral of the ACP region, whereas the blue squares denoted the signal integral of the apatite region (see the caption of Fig. S6). Similar results were obtained for other teeth samples. The data were analyzed based on the following equation

$$M(t) = M_0[1 - \exp\left(\frac{-t}{\tau_{cp}}\right)]\exp\left(\frac{-t}{T_{1\rho}}\right)$$

where *t* is the contact time; M_0 denotes the unmodulated signal intensity; τ_{cp} and $T_{1\rho}$ characterize the transfer dynamics. We found that the CP transfer dynamics were critically dependent on the hydration level and the fluoride content of the samples. Consequently, only the comparison of the M_0 ratio of apatite and ACP among the teeth samples are warranted, but not τ_{cp} and $T_{1\rho}$ because ^{19}F decoupling was not applied during the contact time period.

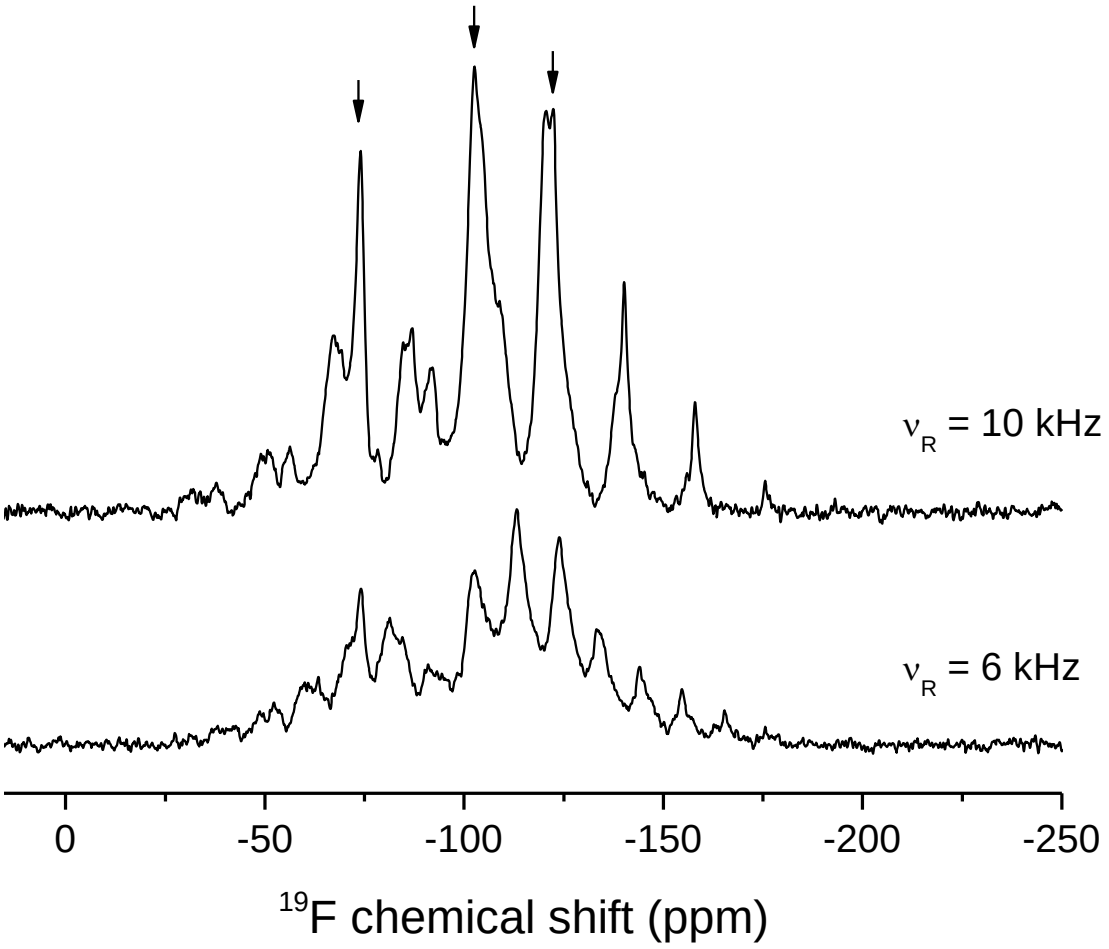

Figure S9. ^{19}F MAS spectra acquired for the oA teeth sample at different spinning frequencies (ν_R). The arrows indicate the positions of the center bands of the three distinctive signals. Other peaks correspond to the spinning sidebands.

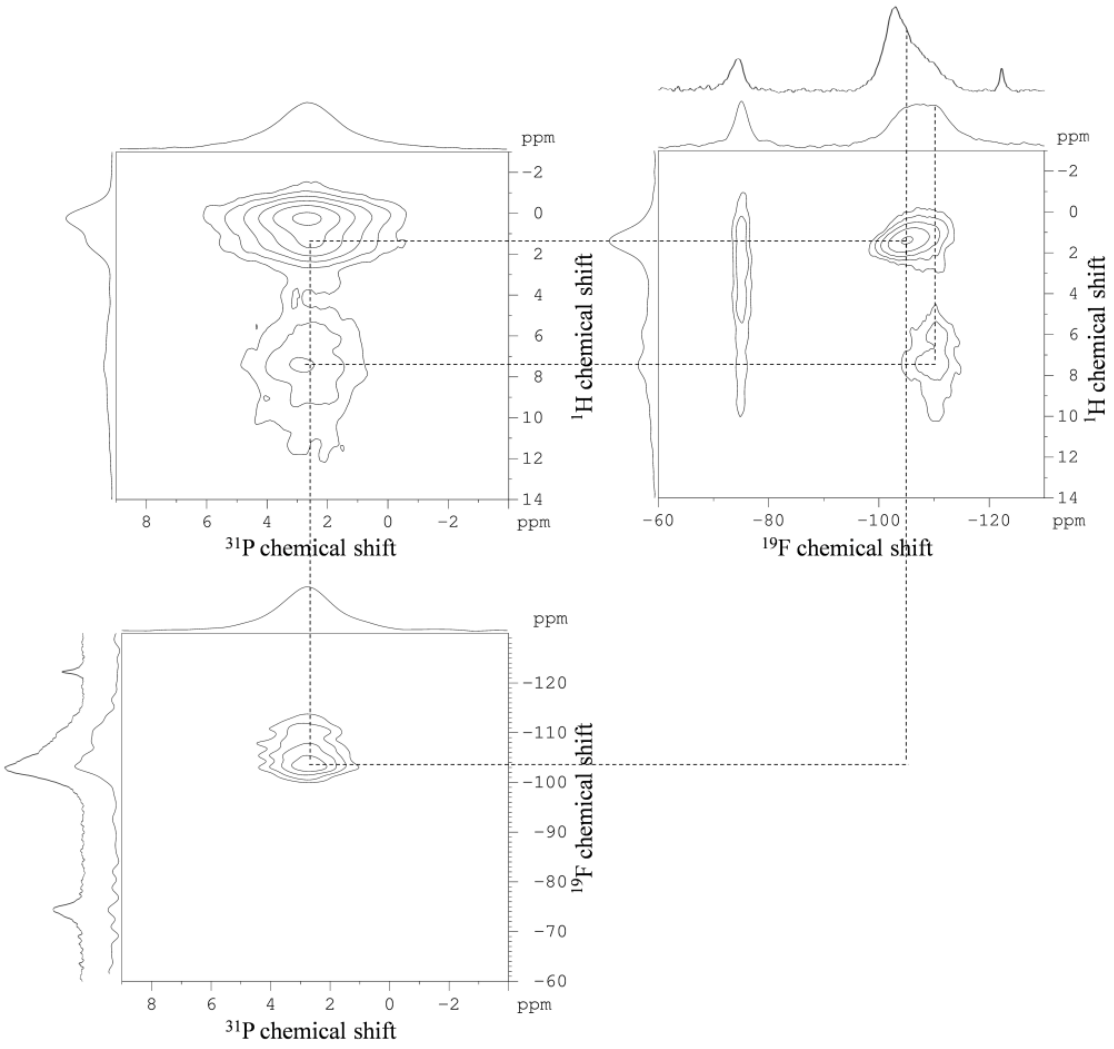

Figure S10. $^{31}P\{^{1}H\}$, $^{19}F\{^{1}H\}$, and $^{31}P\{^{19}F\}$ HETCOR spectra acquired for the oA sample. The traces on top of the projections represent the corresponding 19F MAS spectrum (direct polarization).

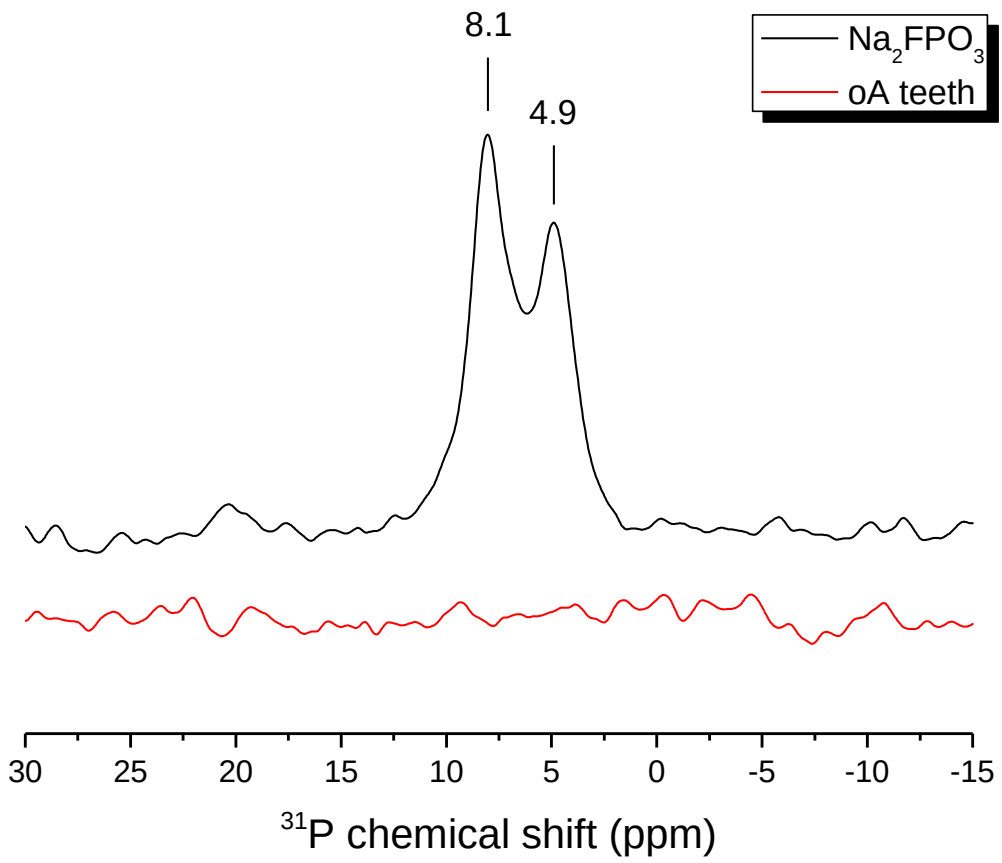

Figure S11. $^{31}P\{^{19}F\}$ TEDOR spectra acquired for disodium monofluorophosphate and the oA samples. The number of transients accumulated for Na_2FPO_3 and oA were 8 and 2048, respectively. After normalizing by the number of scan, the intensity ratio of the signals of the shark teeth to Na_2FPO_3 was 1.6×10^{-3}. The sample masses of the shark teeth and Na_2FPO_3 were 9.9 and 21.6 mg, respectively, from which it was estimated that the amount of Na_2FPO_3 in the shark teeth must be less than 0.34 wt%. Our estimation assumed that the Na_2FPO_3 in shark teeth, if any, did not have any motional dynamics nor chemical exchange. In our TEDOR measurements, the ^{19}F polarization was excited by a single $\pi/2$ pulse.

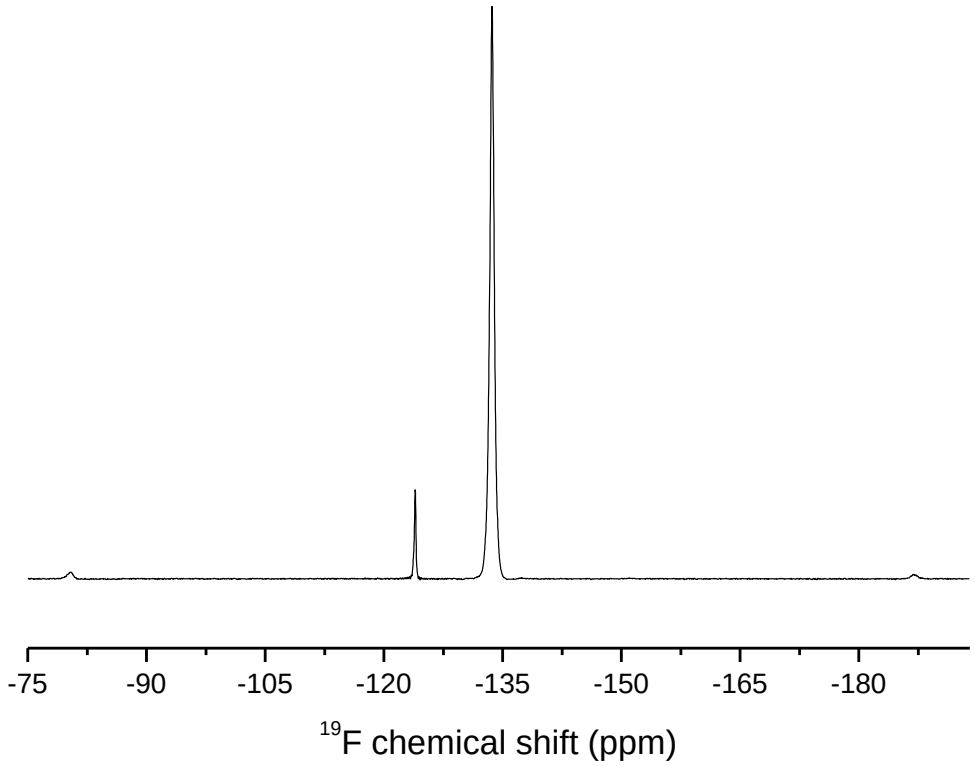

Figure S12. ^{19}F MAS spectrum of potassium fluoride under a spinning frequency of 30 kHz.

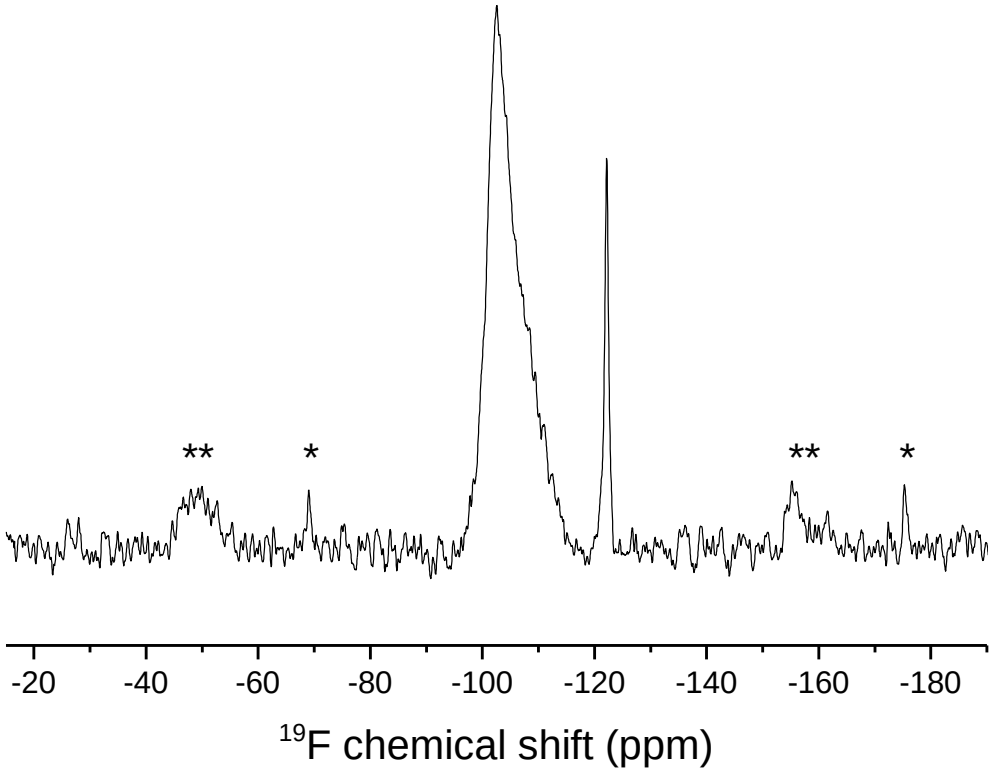

Figure S13. ^{19}F MAS spectrum acquired for the teeth taken from the third series of the anterior region (3A) under a spinning frequency of 30 kHz. The spinning sidebands of the apatite signal were marked with ** and those arising from the signal at –122.2 ppm were marked with *. From the relative sideband intensities, one may infer that the ^{19}F chemical shift anisotropy of the signal at –122.2 ppm is larger than that of crystalline KF (see Fig. S12).

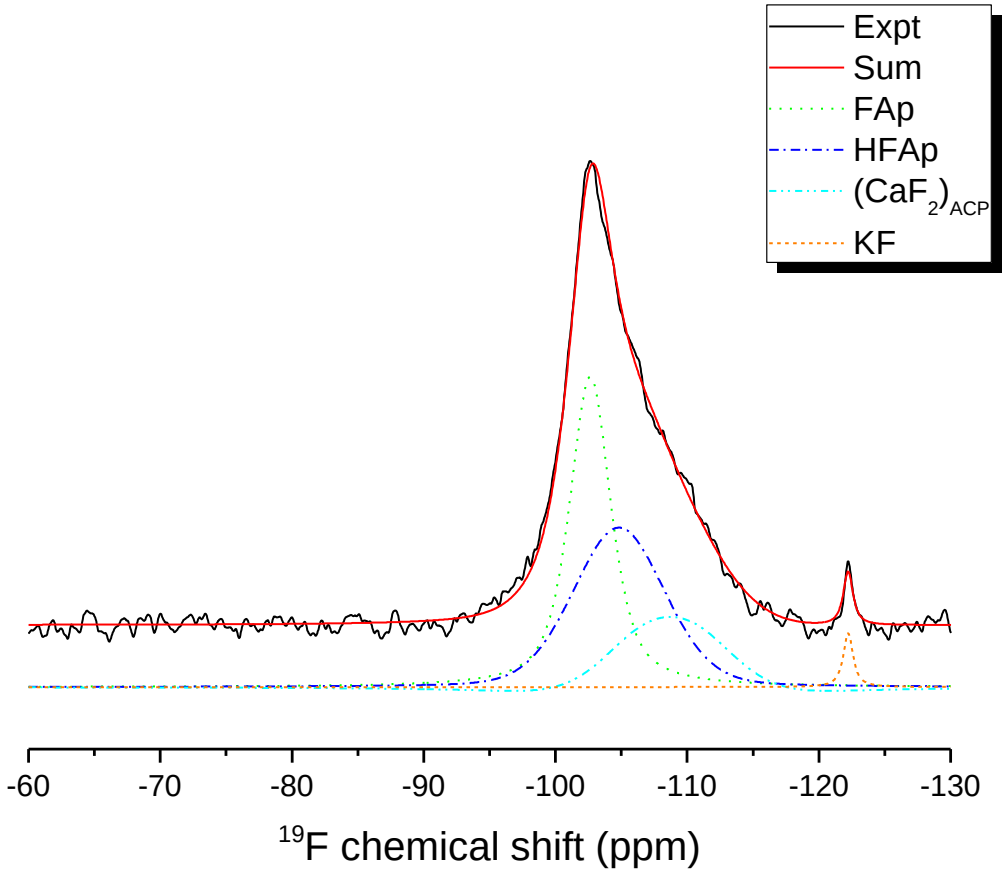

Figure S14. Deconvolution of the 19F MAS spectrum acquired for the teeth taken from the second outer series of the anterior region (2A).

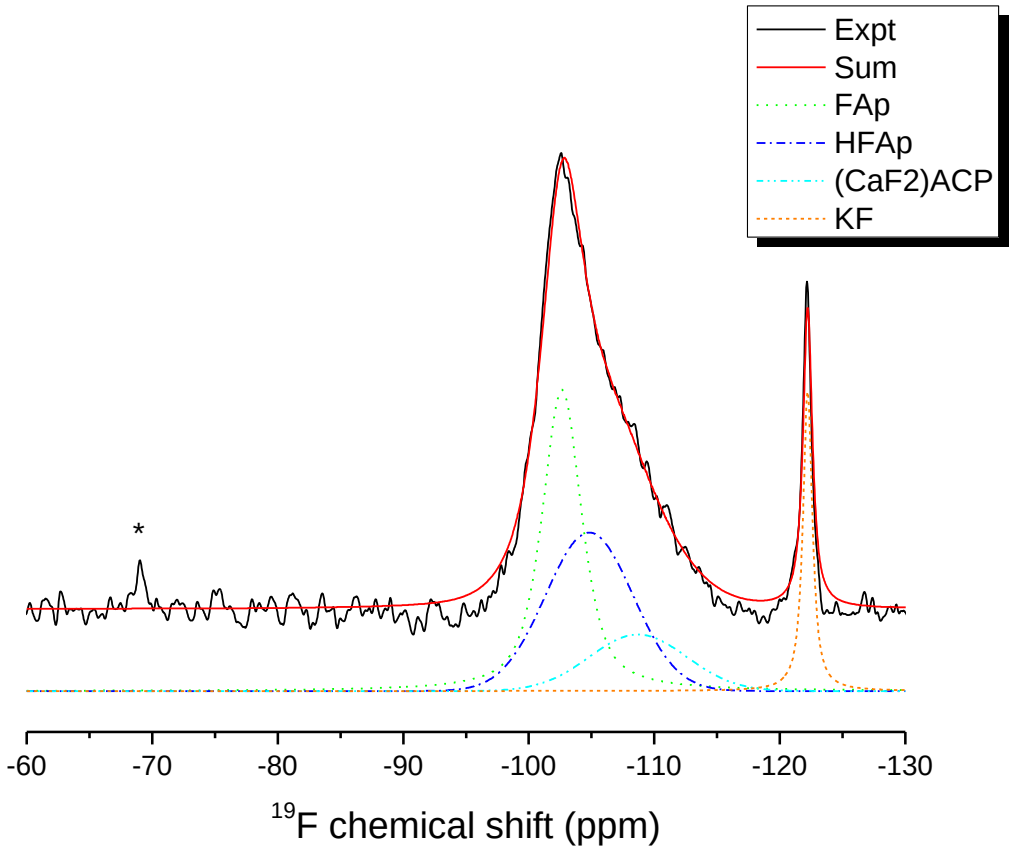

Figure S15. Deconvolution of the 19F MAS spectrum acquired for the teeth taken from the third series of the anterior region (3A). The peak labeled with an asterisk was the spinning sideband of the KF signal.

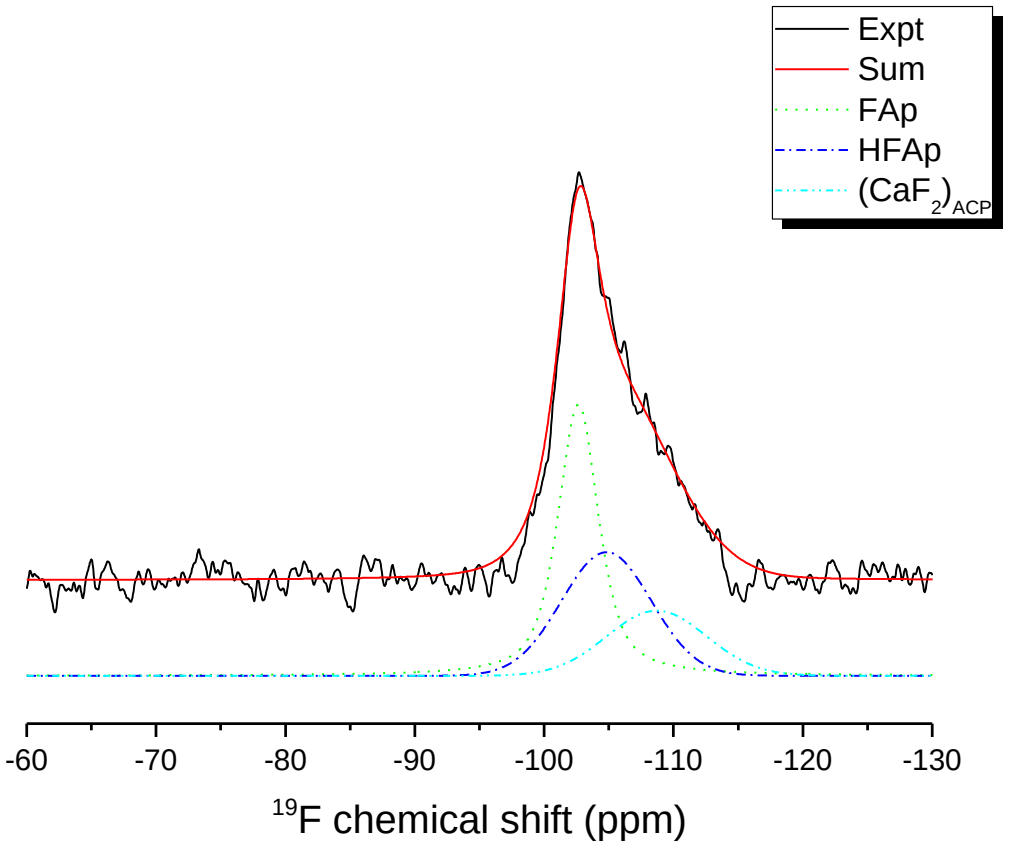

Figure S16. Deconvolution of the 19F MAS spectrum acquired for the teeth taken from the fourth series of the anterior region (4A).

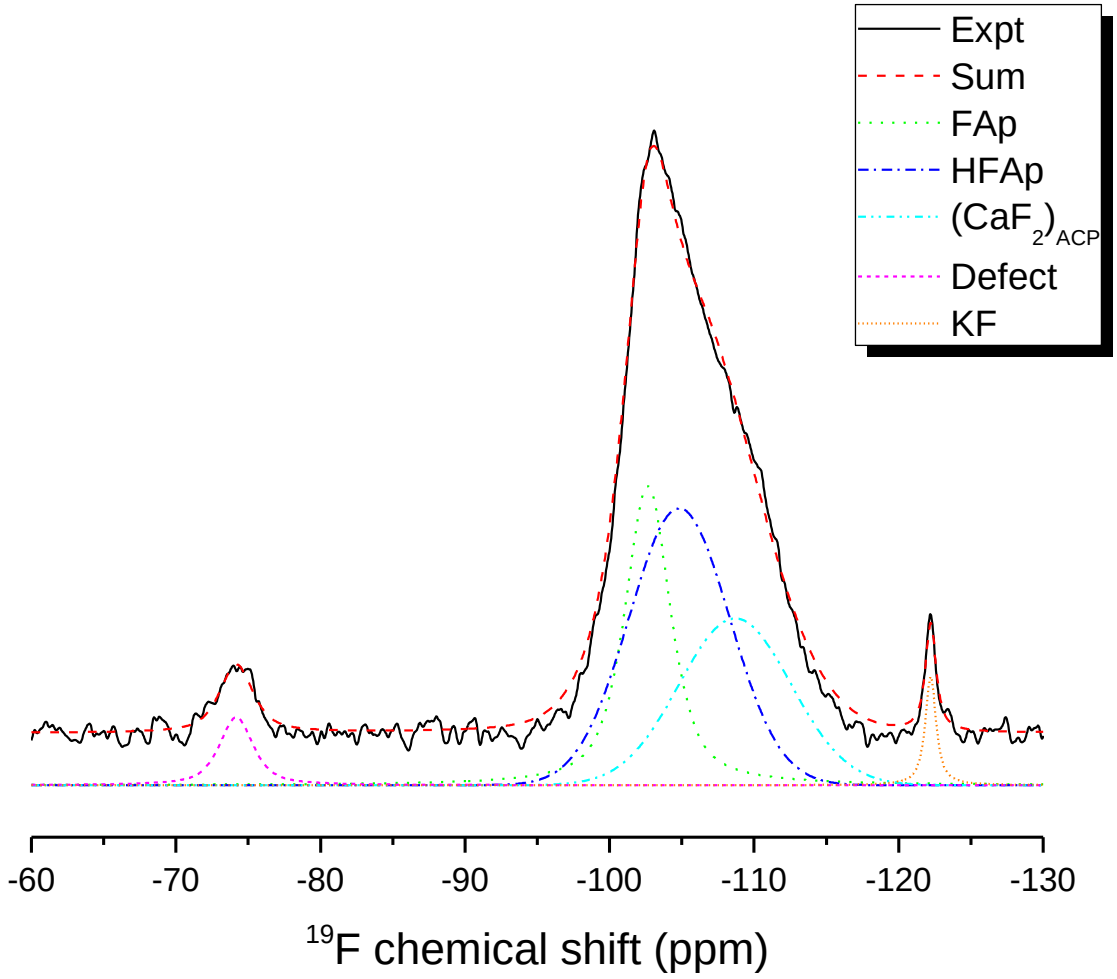

Figure S17. Deconvolution of the 19F MAS spectrum acquired for the teeth taken from the posterior region (P).

3. Table

Table S1. Summary of the results of the variable contact-time $^{13}C\{^{1}H\}$ CPMAS experiments.

		M_0		τ_{cp} (ms)	$T_{1\rho}$ (ms)
HAp		--		1.9 ± 0.1	65 ± 13
oA	Ap	0.98 ± 0.02	66%	1.36 ± 0.06	--
	ACP	0.51 ± 0.01	34%	0.34 ± 0.02	9.5 ± 0.4
2A	Ap	1.02 ± 0.02	62%	1.15 ± 0.05	--
	ACP	0.62 ± 0.01	38%	0.31 ± 0.02	10.0 ± 0.5
3A	Ap	1.07 ± 0.04	58%	1.11 ± 0.10	--
	ACP	0.77 ± 0.04	42%	0.42 ± 0.05	7.7 ± 0.8
4A	Ap	1.18 ± 0.02	60%	1.82 ± 0.07	44 ± 4
	ACP	0.80 ± 0.02	40%	0.44 ± 0.04	19.7 ± 1.4
P	Ap	1.26 ± 0.07	66%	1.7 ± 0.2	30 ± 5
	ACP	0.64 ± 0.03	34%	0.45 ± 0.05	11.1 ± 0.9

Table S2. Summary of the deconvolution results of the ^{19}F MAS spectra acquired for shark teeth and the model compound FAp.

Samples	Mass (mg)	Assignment	Chemical shifts (ppm)	Normalized Intensity*	Mass Percentage (%)
FAp	18.3†	FAp	−102.5	759.2	100
oA	7.3	Defect	-74.2	7.96	2.63 ± 0.06
		FAp	-102.6	14.37	4.7 ± 0.3
		HFAp	-104.8	19.26	6.4 ± 0.6
		$(CaF_2)_{ACP}$	-108.7	8.02	0.21 ± 0.02
		KF	-122.2	1.84	0.070 ± 0.004
2A	6.7	--	--	--	--
		FAp	-102.6	22.15	8.0 ± 0.6
		HFAp	-104.8	21.10	7.6 ± 0.8
		$(CaF_2)_{ACP}$	-108.7	7.84	0.22 ± 0.02
		KF	-122.2	1.02	0.042 ± 0.002
3A	6.6	--	--	--	--
		FAp	-102.6	16.30	6.0 ± 0.4
		HFAp	-104.8	14.88	5.4 ± 0.6
		$(CaF_2)_{ACP}$	-108.7	5.90	0.17 ± 0.02
		KF	-122.2	4.31	0.181 ± 0.009
4A	3.9	--	--	--	--
		FAp	-102.6	12.34	7.6 ± 0.6
		HFAp	-104.8	9.92	6.1 ± 0.6
		$(CaF_2)_{ACP}$	-108.7	5.81	0.28 ± 0.03
		--	--	--	--
P	6.6	Defect	-74.2	1.09	0.40 ± 0.02
		FAp	-102.6	6.37	2.3 ± 0.2
		HFAp	-104.8	10.23	3.7 ± 0.4
		$(CaF_2)_{ACP}$	-108.7	6.86	0.19 ± 0.02
		KF	-122.2	0.61	0.026 ± 0.001

† The contribution of the minor phases of HFAp and CaF_2 to the sample mass has been deducted.

* Intensities were normalized by the number of scan. The minor contributions from the spinning sidebands were not included.

Table S3. Summary of the potassium ICP-MS data acquired for selected shark teeth.[†]

Samples	sample mass (mg)	K-39 (ppb)	KF weight %
2A	2.8 ± 0.1	158.3 ± 3.6	0.085 ± 0.003
3A	3.4 ± 0.1	595.0 ± 2.9	0.26 ± 0.01

[†] Each sample was dissolved in 10 mL of 3% HNO_3 solution.

4. References

1 A. E. Bennett, C. M. Rienstra, M. Auger, K. V. Lakshmi and R. G. Griffin, *J. Chem. Phys.*, 1995, **103**, 6951–6958.

2 A. Hing, S. Vega and J. Schaefer, *J. Magn. Reson.*, 1992, **96**, 205–209.

3 H. Ou-Yang, E. P. Paschalis, A. L. Boskey and R. Mendelsohn, *Biopolymers*, 2000, **57**, 129–139.

4 D. W. Kim, I. S. Cho, J. Y. Kim, H. L. Jang, G. S. Han, H. S. Ryu, H. Shin, H. S. Jung, H. Kim and K. S. Hong, *Langmuir*, 2010, **26**, 384–388.

5 B. J. MacFadden, L. R. G. DeSantis, J. L. Hochstein and G. D. Kamenov, *Palaeogeogr. Palaeoclimatol. Palaeoecol.*, 2010, **291**, 180–189.

6 A. P. Kumar, K. K. Mohaideen, S. A. S. Alariqi and R. P. Singh, *Macromol. Res.*, 2010, **18**, 1160–1167.

7 H. U. V. Gerth, T. Dammaschke, E. Schafer and H. Zuchner, *Dent. Mater.*, 2007, **23**, 1521–1528.